Beyond the Physico-Chemical Barrier: Glycerol and Xylitol Markedly yet Differentially Alter Gene Expression Profiles and Modify Signaling Pathways in Human Epidermal Keratinocytes

Edit Páyer[1,2,3,*], Judit Szabó-Papp[1,2,*], Lídia Ambrus[1,4], Attila Gábor Szöllősi[1], Mónika Andrási[5], Shabtay Dikstein[6], Lajos Kemény[7], István Juhász[2], Andrea Szegedi[2], Tamás Bíró[4,**], Attila Oláh[1,**]

Departments of [1]Physiology, [2]Dermatology, [3]Internal Medicine, [4]Immunology, and [5]Surgery, Faculty of Medicine, University of Debrecen, Debrecen, Hungary

[6]School of Pharmacy, The Hebrew University, Jerusalem, Israel

[7]MTA-SZTE Dermatological Research Group, Department of Dermatology and Allergology, University of Szeged, Szeged, Hungary

*: shared first authorship

**: shared corresponding authorship

Correspondence should be addressed to:

Tamás Bíró (University of Debrecen, Nagyerdei krt. 98. Debrecen, H-4032, Hungary; e-mail: biro.tamas@med.unideb.hu).

SUPPLEMENTARY DATA

SUPPLEMENTARY BACKGROUND

Importantly, glucose-derived glycerol is endogenously synthesized in the skin (mostly in the sebaceous glands) and was suggested to play a crucial role in the homeostatic regulation of the skin barrier (4,6-8). Indeed, in asebia mice with impaired sebaceous gland functions and hence a dramatically suppressed (by 85%) endogenous glycerol production, decreased SC hydration was observed which was completely reverted by application of exogenous glycerol (7). Likewise, hydration in the human skin was also found to be correlated with endogenous glycerol levels in the SC (9). Therefore, it is proposed that the highly beneficial effects of topically applied glycerol in a multitude of skin conditions (e.g. dry skin syndromes such as winter xerosis, irritative skin syndromes, dermatoses with impaired barrier, atopic dermatitis, etc.) is due to its “replacement actions” by normalizing endogenous glycerol-controlled homeostatic cutaneous mechanisms.

The cutaneous effects of glycerol were mostly (if not exclusively) attributed to its physico-chemical properties. Endogenously produced or exogenously applied glycerol penetrates to keratinocytes located in the basal layer(s) of the epidermis via aquaglyceroporin AQP3 pores and, due to its humectancy or hygroscopicity, promotes the establishment and maintenance of the epidermal barrier (4-6,8). Indeed, in AQP3-deficient mice with decreased SC hydration and pathological barrier (4,10), application of glycerol improved skin hydration and accelerated barrier recovery (8).

SUPPLEMENTARY EXPERIMENTAL DESIGN

Cell culturing

Human abdominal skin samples were collected after written informed consent from dermatologically healthy individuals (18-73 years old females and males), undergoing surgical intervention, adhering to Helsinki guidelines and after obtaining Institutional Research Ethics Committee's and National Public Health and Medical Officer Service - Office of the Chief Medical Officer's permission (protocol No.: *DE OEC RKEB/IKEB 3724-2012*; document No.: *IX-R-052/01396-2/2012*). NHEKs were isolated after overnight dermo-epidermal separation in 2.4 IU/ml dispase (Roche Diagnostics, Berlin, Germany) by short trypsin (0.05%, Sigma-Aldrich, St. Louis, MO) digestion. Cells were cultured in EpiLife serum free medium (Invitrogen, Paisley, UK) supplemented with 1 μM insulin, 1 μM cortisol (both from Sigma-Aldrich), 100 μg/ml streptomycin, 100 U/ml penicillin, 50 ng/ml amphotericin B, 0.4% bovine pituitary extract (all from Invitrogen) and 0.06 mM $CaCl_2$ (Sigma-Aldrich) (21). In order to achieve "pre-confluent" cultures, 500,000 cells were seeded in 35 mm Petri dishes, and the appropriate treatments were initiated on the day after, whereas in case of those cultures, which were to be investigated in post-confluent state, culture medium was exchanged daily until the cultures reached 100% confluence (i.e. for ca. 3-4 days), when the indicated treatments were executed. In each experiment, cells of the same donor were used for both the pre- and the post-confluent experiments.

Overview of the TLR-activation-induced pro-inflammatory models

Lipopolysaccharide (LPS; TLR4 activator), lipoteichoic acid (LTA; TLR2 activator) and polyinosinic-polycitidylic acid (poly-(I:C); TLR3 activator) were dissolved in filtered distilled water; all substances were purchased from Sigma-Aldrich. Pre-

confluent cultures of NHEKs were treated with these substances w/wo glycerol or xylitol for 3 hrs (simultaneous treatments), and then RNA samples were collected for subsequent analyses.

Determination of viability

The viability was determined by measuring the conversion of the tetrazolium salt (methylthiazolyldiphenyl-tetrazolium bromide, MTT; Sigma-Aldrich) to formazan by mitochondrial dehydrogenases (21,22). Cells were plated in 96-well plates (10,000 cells/well density) in quadruplicates, and were treated with xylitol (0.0045-0.45%) or glycerol (0.0027-0.27%) for various time intervals. Cells were then incubated with 0.5 mg/ml MTT for 2 hrs, and concentration of formazan crystals was determined colorimetrically according to the manufacturer's protocol.

Determination of cell death

A decrease in the mitochondrial membrane potential is one of the earliest markers of apoptosis. Therefore, to assess the process, mitochondrial membrane potential of NHEKs was determined using a MitoProbe™ $DiIC_1(5)$ Assay Kit (Life Technologies, Carlsbad, CA, USA). Cells (20,000 cells/well) were cultured in 96-well black-well/clear-bottom plates (Greiner Bio One, Frickenhausen, Germany) in quadruplicates and were treated with various compounds. After removal of supernatants, cells were incubated for 30 minutes with $DiIC_1(5)$ working solution (50 µl/well), then washed with PBS (115 mM NaCl, 206 mM Na_2PO_4, pH 7.4; all from Sigma-Aldrich), and the fluorescence of $DiIC_1(5)$ was measured at 630 nm excitation and 670 nm emission wavelengths using a FlexStation 3 FLuorescence Image MicroPlate Reader (FLIPR; Molecular Devices, San Francisco, CA).

Necrotic processes were determined by SYTOX Green staining (Life Technologies). The dye is able to penetrate (and then bind to the nucleic acids) only to necrotic cells with ruptured plasma membranes, whereas healthy cells with intact surface membranes show negligible SYTOX Green staining. Cells were cultured in 96-well black-well/clear-bottom plates (Greiner Bio One), and treated with polyols. Supernatants were then discarded, and the cells were incubated for 30 minutes with 1 μM SYTOX Green dye. Following incubation, cells were washed with PBS, the culture medium was replaced, and fluorescence of SYTOX Green was measured at 490 nm excitation and 520 nm emission wavelengths using FLIPR (Molecular Devices) (21,22).

Quantitative Real-Time PCR (Q-PCR)

To determine the quantitative expressions of various markers at the mRNA level, Q-PCR was performed on an ABI Prism 7000 sequence detection system (Applied Biosystems, Foster City, CA) using the 5' nuclease assay as detailed in our previous reports (21-24). In brief, total RNA was isolated using TRIzol (Invitrogen) and 3 μg of total RNA were reverse-transcribed into cDNA by using 15 IU of AMV reverse transcriptase (Promega, Madison, WI, USA) and 0.025 μg/μl random primers (Promega). PCR amplification was performed by using TaqMan primers and probes (Applied Biosystems). As internal controls, transcripts of cyclophilin A (PPIA) were determined. Assay ID-s of the applied primer probes are overviewed in **Supplementary Table S1**.

Western blotting

To determine the activation of the Erk1/2 MAPK, as well as the expressional alteration of loricrin at the protein level, the Western blot technique was applied (22,25). Cell lysates of keratinocytes were subjected to sodium dodecyl sulfate-polyacrylamide gel electrophoresis (8% gels were loaded with 30 μg protein per lane), transferred to BioBond nitrocellulose membranes (Whatman, Maidstone, UK), and then probed with primary antibodies against loricrin, Erk1/2 and phospho-Erk1/2 (1:500, all from Sigma-Aldrich). A horseradish peroxidase-conjugated IgG antibody (1:1000, Bio-Rad, Hercules CA, USA) was used as a secondary antibody, and the immunoreactive bands were visualized by a SuperSignal® West Pico Chemiluminescent Substrate enhanced chemiluminescence kit (Pierce, Rockford, IL, USA) using LAS-3000 Intelligent Dark Box (Fuji, Tokyo, Japan). In case of loricrin, to assess equal loading, membranes were re-probed with an anti-β-actin antibody (1:2000, Santa Cruz, CA, USA) and visualized as described above. Immunoblots were then subjected to densitometric analysis using an Intelligent Dark Box (Fuji, Tokyo, Japan) and the *ImageJ 1.49v* software (NIH, Bethesda, MD, USA). In case of Erk1/2 activation 100 nM phorbol 12-myristate 13-acetate (PMA; Sigma-Aldrich) was employed as positive control.

Ca^{2+}-imaging

Changes in intracellular calcium concentration ($[Ca^{2+}]_i$) upon applications of the polyols were detected by fluorimetric Ca^{2+}-imaging (21,26,27). Cells were seeded in 96-well black-well/clear-bottom plates (Greiner Bio One) at a density of 10,000 cells/well and then were incubated with culturing medium containing the cytoplasmic calcium indicator 2 μM Fluo-4 AM (Invitrogen) at 37°C for 40 min. The cells were

washed four times with and finally kept in Hank's solution containing 1% bovine serum albumin and 2.5 mM Probenecid (both from (Sigma-Aldrich) for 30 min at 37 °C. The plates were then placed to FLIPR (Molecular Devices) and changes in $[Ca^{2+}]_i$ (reflected by changes fluorescence; lEX=494 nm, lEM=516 nm) induced by the indicated treatments were recorded in each well.

Immunocytochemistry, confocal microscopy

Human keratinocytes, seeded and cultured on sterile coverslips in 24-well plates, were fixed in acetone, permeabilized by 0.1% Triton-X-100 (Sigma-Aldrich), and then incubated with rabbit primary antibodies against PKCα (Sigma-Aldrich) or PKCδ (Santa Cruz) (1:200 dilution in both cases). For fluorescence staining, slides were then incubated with fluorescein-isothiocyanate (FITC) conjugated secondary antibodies (dilution 1:200, Vector Laboratories, Burlingame, CA, USA) and the nuclei were visualized using DAPI (Vector Laboratories). In course of the optimization of the staining protocols, as negative controls, the appropriate antibody was either omitted from the procedure or was pre-incubated with synthetic blocking peptides (data not shown); for details, see our previous studies (27,28).

To assess the translocation of the PKC isoforms (reflecting activation of the enzymes), the above labeling was performed on cells which were previously treated by 0.27% glycerol or 0.45% xylitol for various time intervals. FITC-labeled cells were then subjected to a visualization procedure using a Zeiss LSM 510 confocal microscopy (Oberkochen, Germany) (25).

Statistical analysis

When applicable, data were analyzed using Student's unpaired, two-tailed *t*-test and $P<0.05$ values were regarded as significant differences.

SUPPLEMENTARY CONCLUSIONS

Here we provide the first evidence that glycerol and xylitol exert profound effects on gene expressions and the activities of various signaling pathways of NHEKs. The observed differential effects of xylitol and glycerol are astounding, since both polyols have high water sorption capacity (7). However, since these two polyols exerted different effects when applied at identical osmolarities, we propose that some of their actions may be mediated not exclusively by their physico-chemical properties.

First, we showed that both polyols (without affecting viability of the cells; **Supplementary Figure S1**) significantly up-regulated the expression of various differentiation markers (**Figure 1**). Indeed, both glycerol and xylitol markedly upregulated expression of filaggrin and loricrin, key molecules of the epidermal barrier (30,s1), both in the proliferating and differentiating keratinocytes (**Figure 1**). Likewise, both polyols significantly increased the expression of occludin (**Figure 1**), an important molecule in the formation of epidermal barrier junctions (s2,s3). Interestingly, only xylitol was able to significantly upregulate the level of involucrin (**Figure 1**), another key molecule participating in epidermal differentiation. These findings collectively implicate that the cutaneous barrier-repairing and differentiation-promoting effects of xylitol might be superior to those of glycerol. Interestingly, however, when tested at the protein level, glycerol appeared to be more efficient than xylitol in upregulating loricrin expression in already differentiating NHEKs (48-hr treatments; **Supplementary Figure S2**). Although data of this pilot experiment performed on cells of one single donor await to be confirmed on multiple donors, they highlight that i) cellular effects of the polyols may well be donor-dependent ones; and ii) mRNA level findings cannot necessarily be directly translated to the protein level.

In a wider sense, it is interesting to note that the gylcerol-conducting pore AQP3 is expressed at the basolateral membrane of colonic epithelial cells, too, and its knockdown caused a dramatic, dose-dependent increase in *E. coli C25* translocation, with the reduction of transepithelial electrical resistance (TEER) and increasing LY (a fluorescent dye) permeability. Of great importance, expression of claudin-1 and occludin were significantly decreased in the AQP3 knockdown group, demonstrating that knockdown of AQP3 (maybe leading to inappropriate glycerol uptake and signaling?) might impair the intestinal barrier integrity via dysregulating occludin expression (s4). On the other hand, cellular effects of glycerol might even be dose-dependently opposing ones, since an injection of high dose (10%) glycerol solution led to an overall suppression of spermatogenesis in rats. Importantly, an equi-osmolar solution of glucose also resulted in significant suppression of spermatogenesis, but the effect of glycerol was significantly greater, suggesting a mechanism in addition to hyperosmolarity (s5), and indeed, in a more recent study, glycerol treatment disrupted tight junction-associated F-actin and occludin and tubulin organization in rat Sertoli cells (s6).

Interestingly, similarities and differences were also observed when we attempted to uncover the effects of the polyols on the cellular signaling pathways known to be involved in the regulation of epidermal growth and differentiation. As revealed by functional imaging, neither polyol altered the intracellular calcium homeostasis of the cells (**Supplementary Figure S3**). This implies that their pro-differentiating effects are most probably not mediated by the elevation of $[Ca^{2+}]_i$, which is one of the key events in the induction of terminal differentiation of epidermal keratinocytes (35). The

lack of the involvement of $[Ca^{2+}]_i$ was also suggested by that neither polyol affected subcellular localization of the calcium-dependent PKCα (reflecting lack of activation; **Supplementary Figure S4**), which enzyme was shown to be involved in the $[Ca^{2+}]_i$-mediated differentiation of NHEKs (36). However, xylitol (but not glycerol) was able to induce the translocation of the Ca^{2+}-independent PKCδ (**Figure 2A**). Since we have previously shown that (similar to PKCα) PKCδ promoted differentiation of human epidermal keratinocytes (37), this intriguing finding suggested that the more pronounced pro-differentiating and barrier-promoting effect of xylitol over glycerol might have been mediated by the additional involvement of PKCδ-coupled signaling. Finally, we have also presented that both polyols activated the Erk1/2 MAPK pathway (**Figure 2B**), another molecular system controlling keratinocyte growth and survival (38,39).

Of further importance, differential effects of the two polyols could also be identified when we assessed their actions in various TLR-mediated inflammation (40) and irritation keratinocyte models (**Supplementary Tables S2-S10**). Although their efficiencies were found to be donor- and cytokine-dependent ones, and xylitol appeared to be more potent in most cases, we found that both polyols could prevent TLR-activation-induced upregulation of several pro-inflammatory cytokines (IL-1α, IL-1β, TNFα). Moreover, both glycerol and xylitol decreased the up-regulation of HLA-DR, a marker of immune activation (41,42).

Although our current data provide an important new insight to the mechanism of action of these polyols (activation of the MAPK cascade by both of them; activation of PKCδ by xylitol), it should also be noted that since glycerol (and in low amounts even

xylitol) can be produced in the human body, it is possible that administration of such compounds exerts biological effects not only via their physicochemical properties, and activation/inhibition of several cellular signaling pathways, but they might also have a direct biochemical impact on the cellular metabolism and (at least *in vivo*) even on the microbiota-skin cross-talk, too.

Supplementary Tables

Supplementary Table S1 *Overview of the primer probes used for the Q-PCR analyses*

Gene symbol	***Gene name***	***Assay ID***
FLG	Filaggrin	Hs00856927_g1
LOR	Loricrin	Hs01894962_s1
IVL	Involucrin	Hs00846307_s1
OCLN	Occludin	Hs00170162_m1
HLA-DRA	Major histocompatibility complex, class II, DR alpha	Hs00219575_m1
IL1α	Interleukin 1α	Hs00174092_m1
IL1β	Interleukin 1β	Hs00174097_m1
IL6	Interleukin 6	Hs00985639_m1
IL8	Interleukin 8	Hs00174103_m1
IL18	Interleukin 18	
TNFα	Tumor necrosis factor α	Hs00174128_m1
MMP1	Matrix metalloproteinase 1	Hs00899658_m1
MMP9	Matrix metalloproteinase 9	Hs00234579_m1
PPIA	Peptidylprolyl Isomerase A (cyclophilin A)	Hs99999904_m1

Supplementary Tables (ST) S2-S10 *Effects of polyols on expressions of various inflammation markers*

Keratinocytes from nine donors were treated with various TLR activators – i.e. 10 µg/ml lipoteichoic acid (LTA, TLR2 activation model); 20 µg/ml polyinosinic:polycytidylic acid (poly-IC, pIC; TLR3 activation model); 5 µg/ml lipopolysaccharide (LPS, TLR4 activation model) – with or without glycerol (0.27%) and xylitol (0.45%). The mRNA expressions of multiple pro-inflammatory interleukins (IL), tumor necrosis factor-α (TNFa), and matrix metalloproteases (MMP) as well as the keratinocyte immunoactivation marker HLA-DR were then assessed by Q-PCR. Data were analyzed using the ΔΔCT method. Tables present PPIA-normalized fold-change values where the value of the vehicle control was set as 1. Data represent triplicate determinations in each experiment.

Green font, green background: significant (P<0.05) down-regulation compared to the respective inducer agent (LTA, pIC or LPS) treated group.
Black font, yellow background: tendencies towards down-regulation.
Red font, white background: tendencies towards up-regulation.
Red font, red background: significant (P<0.05) up-regulation compared to the respective inducer agent (LTA, pIC or LPS) treated group.
N/D: not determined
U/I: unidentified
Not induced: ≤1.5-fold up-regulation compared to the control group in the inducer (LTA, pIC or LPS) treated group.

ST2	HLA-DRA								
	Donor 1	Donor 2	Donor 3	Donor 4	Donor 5	Donor 6	Donor 7	Donor 8	Donor 9
ctrl	1	1	1	U/I	U/I	U/I	U/I	U/I	1.00
LPS	Not induced	Not induced	Not induced	U/I	U/I	U/I	U/I	U/I	Not induced
LPS+Gly				U/I	U/I	U/I	U/I	U/I	
LPS+Xyl				U/I	U/I	U/I	U/I	U/I	
LTA	Not induced	1.76	Not induced	U/I	U/I	U/I	U/I	U/I	Not induced
LTA+Gly		1.04		U/I	U/I	U/I	U/I	U/I	
LTA+Xyl		1.05		U/I	U/I	U/I	U/I	U/I	
pIC	Not induced	8.38	2.86	U/I	U/I	U/I	U/I	U/I	Not induced
pIC+Gly		3.76	1.05	U/I	U/I	U/I	U/I	U/I	
pIC+Xyl		1.59	2.00	U/I	U/I	U/I	U/I	U/I	

ST3	IL-1α								
	Donor 1	Donor 2	Donor 3	Donor 4	Donor 5	Donor 6	Donor 7	Donor 8	Donor 9
ctrl	1	1	1	1	1	1	1	1	1
LPS	2.71	Not induced	Not induced	Not induced	1.63	Not induced	Not induced	Not induced	Not induced
LPS+Gly	2.38				1.66				
LPS+Xyl	1.15				1.62				
LTA	3.19	Not induced	2.10	Not induced	1.68	1.99	Not induced	1.64	Not induced
LTA+Gly	3.17		2.13		1.66	1.64		1.94	
LTA+Xyl	1.66		1.47		1.57	1.76		1.57	
pIC	1.86	3.37	1.92	Not induced	1.88	Not induced	2.01	1.98	1.93
pIC+Gly	1.32	3.59	1.33		1.26		2.05	2.19	1.58
pIC+Xyl	1.27	2.40	1.45		1.53		1.97	2.24	2.79

ST4	IL-1β								
	Donor 1	Donor 2	Donor 3	Donor 4	Donor 5	Donor 6	Donor 7	Donor 8	Donor 9
ctrl	1	1	1	1	1	1	1	1	1
LPS	6.91	Not induced	Not induced	Not induced	1.75	Not induced	Not induced	Not induced	Not induced
LPS+Gly	7.62				1.84				
LPS+Xyl	2.41				1.78				
LTA	8.88	1.59	3.17	Not induced	1.93	Not induced	2.36	1.55	1.58
LTA+Gly	10.74	1.86	3.32		1.83		2.14	1.56	1.49
LTA+Xyl	3.74	2.14	3.62		1.75		1.81	1.37	1.52
pIC	4.21	13.44	4.57	Not induced	2.78	Not induced	1.86	2.32	2.59
pIC+Gly	2.90	16.49	4.37		1.11		1.50	2.17	1.75
pIC+Xyl	0.78	9.06	3.83		2.33		2.70	1.83	3.72

ST5	IL-6								
	Donor 1	Donor 2	Donor 3	Donor 4	Donor 5	Donor 6	Donor 7	Donor 8	Donor 9
ctrl	1.00	N/D	1	1	1	1	1	1	1
LPS	Not induced	N/D	Not induced	2.72	1.67	Not induced	Not induced	Not induced	2.42
LPS+Gly		N/D		2.11	2.10				1.88
LPS+Xyl		N/D		2.25	1.14				1.36
LTA	1.86	N/D	Not induced	Not induced	Not induced	Not induced	Not induced	Not induced	Not induced
LTA+Gly	0.90	N/D							
LTA+Xyl	1.69	N/D							
pIC	2.00	N/D	11.88	18.19	115.45	Not induced	7.51	44.43	14.55
pIC+Gly	1.18	N/D	70.92	10.17	177.28		13.13	48.56	5.82
pIC+Xyl	2.17	N/D	12.75	13.70	62.09		6.31	41.87	13.26

ST6	IL-8								
	Donor 1	Donor 2	Donor 3	Donor 4	Donor 5	Donor 6	Donor 7	Donor 8	Donor 9
ctrl	1	N/D	1	1	1	1	1	1	1
LPS	Not induced	N/D	1.82	4.71	1.84	Not induced	4.25	Not induced	Not induced
LPS+Gly		N/D	0.87	5.55	2.74		2.54		
LPS+Xyl		N/D	6.22	6.63	2.47		3.54		
LTA	Not induced	N/D	7.37	1.80	Not induced	Not induced	3.59	2.15	Not induced
LTA+Gly		N/D	38.32	1.96			3.04	2.99	
LTA+Xyl		N/D	54.10	1.44			4.09	2.31	
pIC	Not induced	N/D	241.40	4.51	8.96	1.77	22.09	33.03	12.64
pIC+Gly		N/D	790.02	4.02	12.18	1.94	41.58	41.71	13.46
pIC+Xyl		N/D	531.63	8.91	12.65	2.14	31.57	49.23	16.00

ST7	IL-18								
	Donor 1	Donor 2	Donor 3	Donor 4	Donor 5	Donor 6	Donor 7	Donor 8	Donor 9
ctrl	1	1	1	1	1	1	1	1	1
LPS	11.81	Not induced	1.52	Not induced	Not induced	Not induced	Not induced	Not induced	3.91
LPS+Gly	9.50		1.72						2.70
LPS+Xyl	4.22		2.44						1.79
LTA	5.32	Not induced	1.55	Not induced	Not induced	Not induced	2.54	Not induced	1.54
LTA+Gly	12.19		1.63				2.42		1.58
LTA+Xyl	3.82		2.39				1.96		2.18
pIC	3.08	Not induced	Not induced	Not induced	Not induced	Not induced	Not induced	Not induced	Not induced
pIC+Gly	3.74								
pIC+Xyl	1.30								

ST8	TNFα								
	Donor 1	Donor 2	Donor 3	Donor 4	Donor 5	Donor 6	Donor 7	Donor 8	Donor 9
ctrl	N/D	1	1	N/D	N/D	1	1	1	1
LPS	N/D	Not induced	Not induced	N/D	N/D	Not induced	3.12	1.67	Not induced
LPS+Gly	N/D			N/D	N/D		1.77	1.22	
LPS+Xyl	N/D			N/D	N/D		2.20	1.64	
LTA	N/D	Not induced	Not induced	N/D	N/D	Not induced	1.58	1.65	Not induced
LTA+Gly	N/D			N/D	N/D		1.28	1.79	
LTA+Xyl	N/D			N/D	N/D		1.74	1.99	
pIC	N/D	24.65	14.49	N/D	N/D	1.87	10.87	33.39	12.26
pIC+Gly	N/D	21.88	11.44	N/D	N/D	1.71	10.48	35.28	6.36
pIC+Xyl	N/D	8.86	6.37	N/D	N/D	0.78	11.92	25.37	16.46

ST9	MMP1								
	Donor 1	Donor 2	Donor 3	Donor 4	Donor 5	Donor 6	Donor 7	Donor 8	Donor 9
ctrl	N/D	1	1	N/D	N/D	1	1	1	1
LPS	N/D	Not induced	Not induced	N/D	N/D	Not induced	Not induced	Not induced	Not induced
LPS+Gly	N/D			N/D	N/D				
LPS+Xyl	N/D			N/D	N/D				
LTA	N/D	1.73	5.72	N/D	N/D	Not induced	1.79	Not induced	1.52
LTA+Gly	N/D	1.67	4.97	N/D	N/D		1.08		1.05
LTA+Xyl	N/D	4.18	7.72	N/D	N/D		1.83		1.52
pIC	N/D	3.13	1.59	N/D	N/D	Not induced	Not induced	Not induced	Not induced
pIC+Gly	N/D	2.85	1.22	N/D	N/D				
pIC+Xyl	N/D	3.75	2.26	N/D	N/D				

ST10	MMP9								
	Donor 1	Donor 2	Donor 3	Donor 4	Donor 5	Donor 6	Donor 7	Donor 8	Donor 9
ctrl	N/D	1	1	N/D	N/D	1	1	1	1
LPS	N/D	Not induced	Not induced	N/D	N/D	Not induced	Not induced	Not induced	Not induced
LPS+Gly	N/D			N/D	N/D				
LPS+Xyl	N/D			N/D	N/D				
LTA	N/D	Not induced	Not induced	N/D	N/D	Not induced	1.93	Not induced	Not induced
LTA+Gly	N/D			N/D	N/D		0.64		
LTA+Xyl	N/D			N/D	N/D		1.16		
pIC	N/D	102.69	23.16	N/D	N/D	Not induced	Not induced	Not induced	1.57
pIC+Gly	N/D	149.50	13.47	N/D	N/D				0.96
pIC+Xyl	N/D	29.45	9.22	N/D	N/D				2.33

SUPPLEMENTARY FIGURES

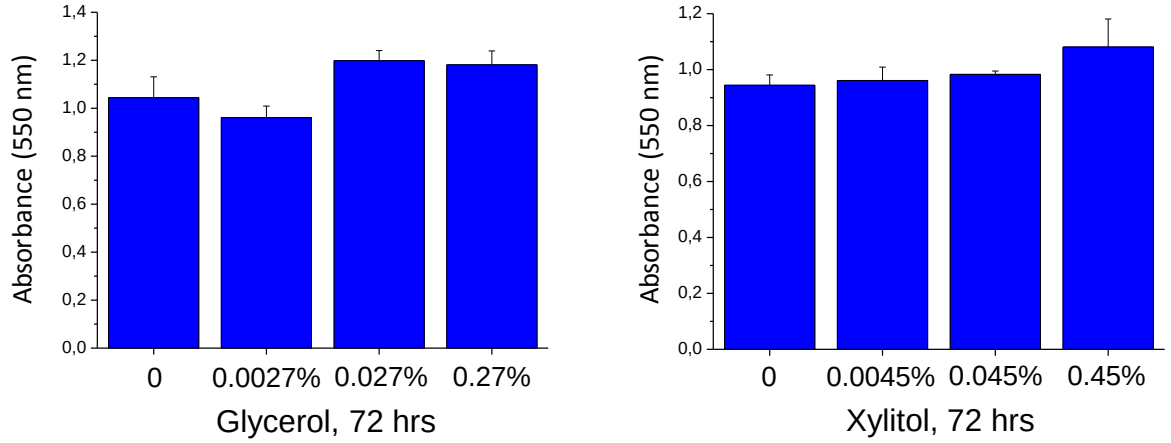

Supplementary Figure S1 *Polyols do not affect viability and proliferation of NHEKs*
Pre-confluent (i.e. proliferating) NHEKs were treated with glycerol and xylitol in quadruplicates as indicated for 72 hrs, and then MTT assays were performed to assess viability and growth rate of the cells. Data are expressed as mean±SEM. Three repeated experiments yielded similar results.

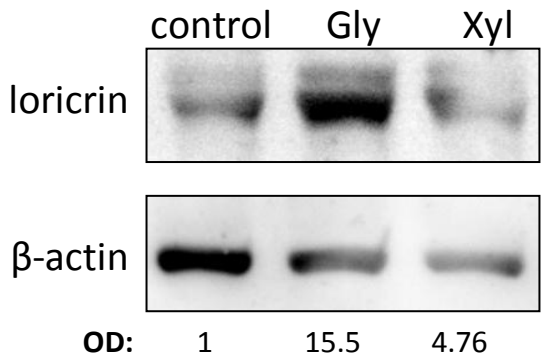

Supplementary Figure S2 *Glycerol up-regulates the expression of loricrin*

Western blot analysis of lysates of post-confluent (i.e. differentiating) NHEKs of one donor. Cells were treated with glycerol (0.27%) and xylitol (0.45%) for 48 hrs, and then the protein level expression of loricrin was assessed (loading control: β-actin). OD: β-actin-normalized optical density of the corresponding bands were normalized to the value of the control group.

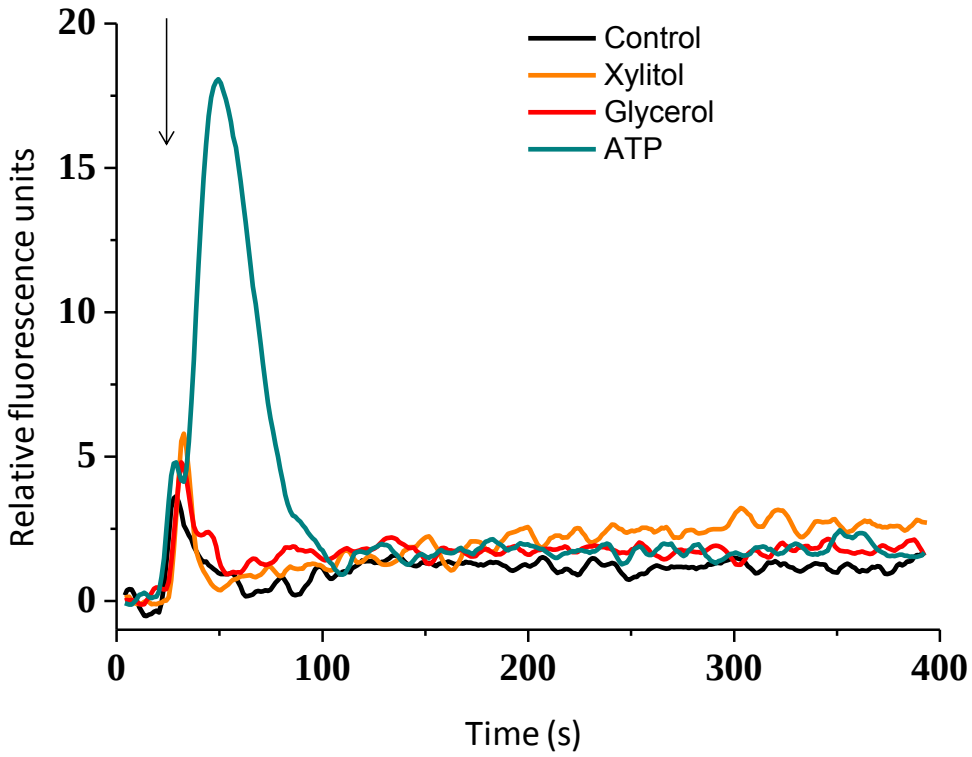

Supplementary Figure S3 *Polyols do not elevate $[Ca^{2+}]_i$ of NHEKs*

Fluorimetric Ca^{2+} imaging using Fluo-4. Glycerol (0.27%) and xylitol (0.45%) were applied as indicated by the arrow. As a positive control, ATP (180 µM) was applied [s7]. Fluorescence (measured in relative fluorescence units) was normalized to the baseline. Two additional series of experiments yielded similar results.

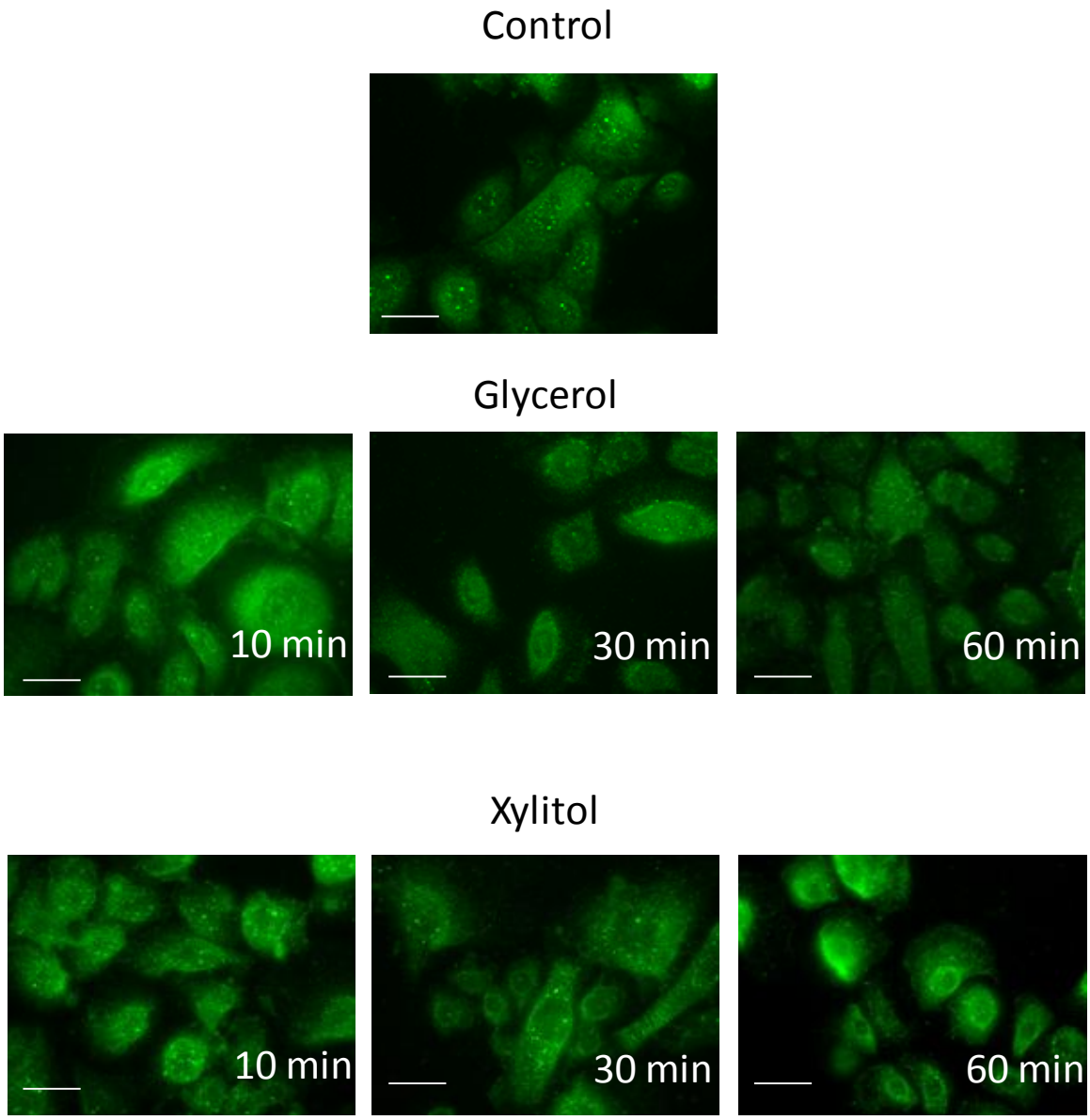

Supplementary Figure S4 *Neither polyol induce the translocation of PKCα in NHEKs*

Confocal microscopy. NHEKs were treated with vehicle (Control) or with Glycerol (0.27%) and xylitol (0.45%) for the time indicated, then immunofluorescent staining of PKCα was performed. Images were acquired by a laser scanning confocal microscope using the “z-stack mode” with strictly the same antibody staining and visualization procedure (the second image from the level of the coverslips). Note the lack of translocation after treatment with polyols. Bars: 10 μm. Two additional experiments yielded similar results.

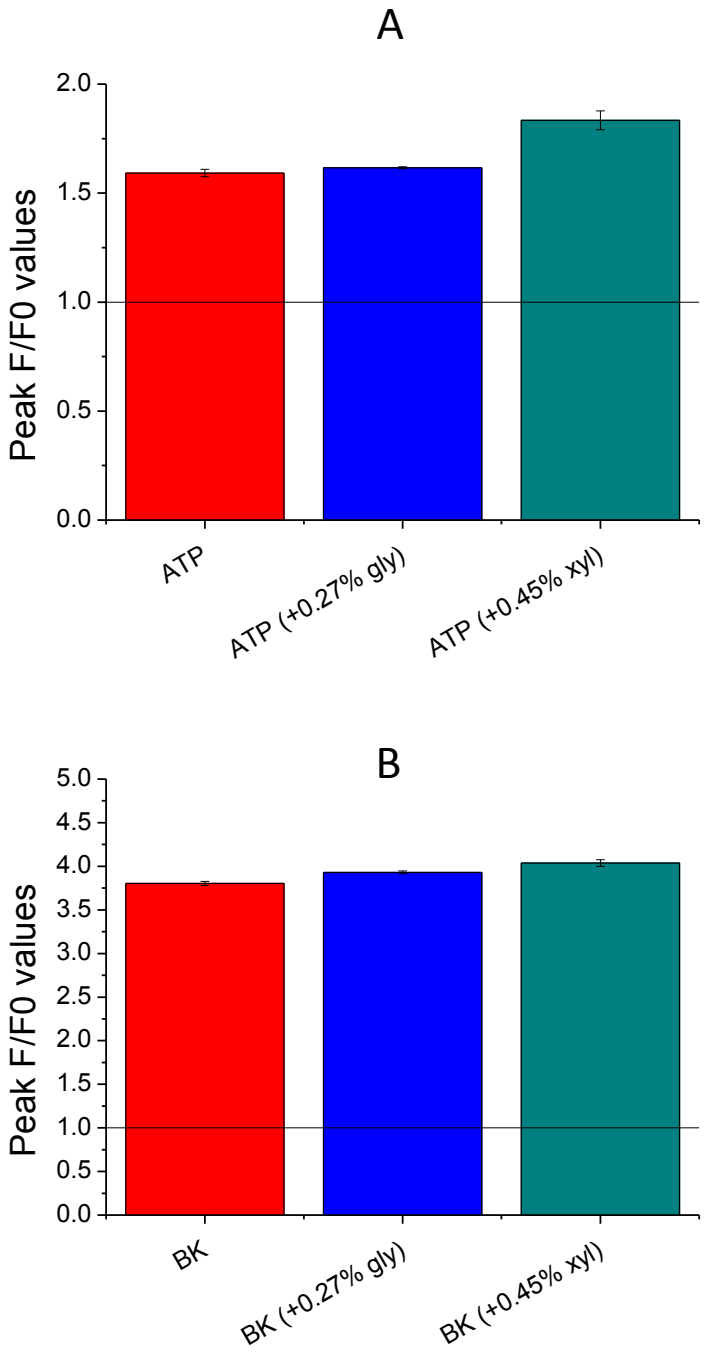

Supplementary Figure S5 *Polyols do not suppress ATP or bradykinin (BK)-induced elevation of $[Ca^{2+}]_i$ of NHEKs*

Fluorimetric Ca^{2+} imaging using Fluo-4. Glycerol (gly; 0.27%) and xylitol (xyl; 0.45%) were applied 30 min before ATP (180 μM) (**A**); or bradykinin (BK 30 μM) (**B**) treatments. Mean±SEM of peak F/F0 values of 6 parallel determinations of one donor are plotted. One additional experiment (performed on cells of an additional donor) yielded similar results.

SUPPLEMENTARY REFERENCES

s1 McAleer M A, Irvine A D. The multifunctional role of filaggrin in allergic skin disease. J Allergy Clin Immunol 2013: **131**: 280–291.

s2 Saitou M, Furuse M, Sasaki H *et al.* Complex Phenotype of Mice Lacking Occludin, a Component of Tight Junction Strands. Mol Biol Cell 2000: **11**: 4131–4142.

s3 Volksdorf T, Heilmann J, Eming S A *et al.* Tight Junction Proteins Claudin-1 and Occludin Are Important for Cutaneous Wound Healing. Am J Pathol 2017: **187**: 1301–1312.

s4 Zhang W, Xu Y, Chen Z *et al.* Knockdown of aquaporin 3 is involved in intestinal barrier integrity impairment. FEBS Lett 2011: **585**: 3113–3119.

s5 Igdoura S A, Wiebe J P. Suppression of spermatogenesis by low-level glycerol treatment. J Androl 1994: **15**: 234–243.

s6 Wiebe J P, Kowalik A, Gallardi R L *et al.* Glycerol disrupts tight junction-associated actin microfilaments, occludin, and microtubules in Sertoli cells. J Androl 2000: **21**: 625–635.

s7 Bíró T, Szabó I, Kovács L *et al.* Distinct subpopulations in HaCaT cells as revealed by the characteristics of intracellular calcium release induced by phosphoinositide-coupled agonists. Arch Dermatol Res 1998: **290**: 270–276.